ELSEVIER

15 May 1998

OPTICS COMMUNICATIONS

Optics Communications 151 (1998) 117–135

Full length article

Variational approach to optical pulse propagation in dispersion compensated transmission systems

S.K. Turitsyn [a,b,1], I. Gabitov [a], E.W. Laedke [a], V.K. Mezentsev [b], S.L. Musher [b], E.G. Shapiro [b], T. Schäfer [a], K.H. Spatschek [a]

[a] *Institut für Theoretische Physik, Heinrich-Heine-Universität Düsseldorf, 40225 Düsseldorf, Germany*
[b] *Institute of Automation and Electrometry, 630090 Novosibirsk, Russia*

Received 29 September 1997; accepted 17 February 1998

Abstract

Within the area of optical pulse propagation in long-haul transmission systems various designs for dispersion compensation are investigated. On the basis of variational procedures with collective coordinates, a very effective method is presented which allows to determine quite accurately the possible operation points. We have obtained an analytical formula for the soliton power enhancement. This analytical expression is in good agreement with numerical results, in the (practical) limit when residual dispersion and nonlinearity only slightly affect the pulse dynamics over one compensation period. The procedure is suitable to analyze the proper design of dispersion compensating elements. The results allow also to describe the shape of the dispersion-managed soliton. We discuss also a qualitative physical explanation of the possibility to transmit a soliton at zero or normal average dispersion. Analytical predictions are confirmed by direct numerical simulations.

1. Introduction

In the past, soliton transmission has already shown its potential in long-haul high-speed communications. Lightwave transmission systems exploiting optical amplifiers to compensate the carrier pulse attenuation in fibers can be used as transoceanic communication links as well as in terrestrial networks. Recent progress in the fabrication of erbium-doped fiber amplifiers has allowed to design several effective variants of long-distance soliton-based optical communication systems (see e.g. Refs. [1–3]).

Solitary pulse propagation in communication systems using low-dispersion fibers is based on the guiding-center (average) soliton concept [1,4–6]. The amplifier spacings Z_a in the transocean lines are shorter than the soliton period, and both dispersion and nonlinearity can be treated as perturbations. Thus, to the leading order, only fiber losses and periodic amplification are significant factors causing amplitude oscillations, while the form of the pulse remains unchanged.

However, most of fiber links installed in Europe are based on standard monomode fibers (SMF) with approximately 17 ps/(nm km) group delay parameter in the third optical window (around 1.55 μm). The problem of upgrading the already installed optical networks is a subject of intensive investigations because of evident practical interest. In conventional transmission systems, point optical amplifiers are usually placed at intervals of a few tens of kilometers. To operate at high bit-rates short solitons are required. For 10 Gb/s transmission at 1.55 μm the associated soliton periods Z_{sol} in SMF are of

[1] E-mail: turitsyn@xerxes.thphy.uni-duesseldorf.de

0030-4018/98/$19.00
PII S0030-4018(98)00109-6

the order of the amplification distance Z_a in the installed European networks [7,8]. The resonance $Z_{sol} \approx Z_a$ causes the generation of radiation and instability of the average soliton propagation.

Chromatic dispersion at 1.55 μm can be diminished (and correspondingly the transmission capacity can be significantly enhanced since the soliton period is inversely proportional to the dispersion) by means of the dispersion compensation technique. For example, the incorporation of a piece of fiber with high normal dispersion reduces the total dispersion of the fiber span between two amplifiers. Recent progress in chirped fiber gratings (see for a review Ref. [9]) allows dispersion of 500 ps/(nm km) (or even more) to be compensated by a grating fiber of a few decimeters in length. Even the use of commercially available dispersion compensating fibers (DCFs) with $D \simeq -(60–80)$ ps/(nm km) leads to a significant network upgrading. Dispersion compensation is a simple and effective technique with many attractive features. It is compatible with the present concept of all-optical transparency of the system, cascadable, and all system components are commercially available.

Dispersion compensation processes were identified in recent experiments [10–12] as promising approaches to increase the transmission capacity in communication systems using SMF, both in unrepeated transmission and cascaded systems. We note also that because DCF has higher losses than SMF, a larger optical gain is required to recover the signal. This leads to additional amplifier noise and some increase in the information error, especially for linear signal transmission. Soliton transmission using the DCF technique has recently attracted more attention [8,13]. Numerical simulations of the soliton transmission in short standard monomode fiber systems, upgraded by dispersion compensation, have been performed in Ref. [8]. It has been shown that 10 Gb/s transmission over 200 km is possible with, e.g., $Z_a = 36$ km amplifier spacing. The DCF pieces allow pulse width recovery after dispersive broadening due to the high dispersion of SMF at 1.55 μm. The large variations of the dispersion lead to oscillations of the pulse width on the amplification distance. The theory of the average pulse propagation in systems using DCF has been presented in Ref. [13]. It has been suggested to use breathing solitons for optical data transmission in SMF at 1.55 μm. 320 Gb/s soliton WDM transmission over 1100 km of SMF with large amplifier spacing of 100 km, using DCF to equalize dispersion, has been demonstrated recently in Ref. [14].

Though dispersion compensation is a natural approach in lines built from SMF, it is also a very promising way to enhance transmission capacity in long-haul lines constructed from DSF. In fact, most of the work on dispersion-managed solitons has concentrated on long-haul systems that use dispersion-shifted optical fibers [15–22]. In the experiments of [15] 60 Gb/s has been transmitted over 10000 km using in-line synchronous modulation and optical filtering with three unequally spaced channels. In a recent experiment [16] 160 Gb/s (8×20 Gb/s) transmission over 4000 km has been achieved using a dispersion flattened fiber [16]. Large variations of local dispersion impose substantial changes in pulse dynamics. Dispersion-managed soliton systems have been studied in a number of publications during the last few years (see e.g. Refs. [8–40]). Numerical simulations and experiments have revealed important features of dispersion-managed solitons. The energy of a dispersion-managed soliton is enhanced in comparison with the fundamental soliton corresponding to the same average dispersion and the same pulse width. Therefore, using dispersion-managed pulses for optical transmission

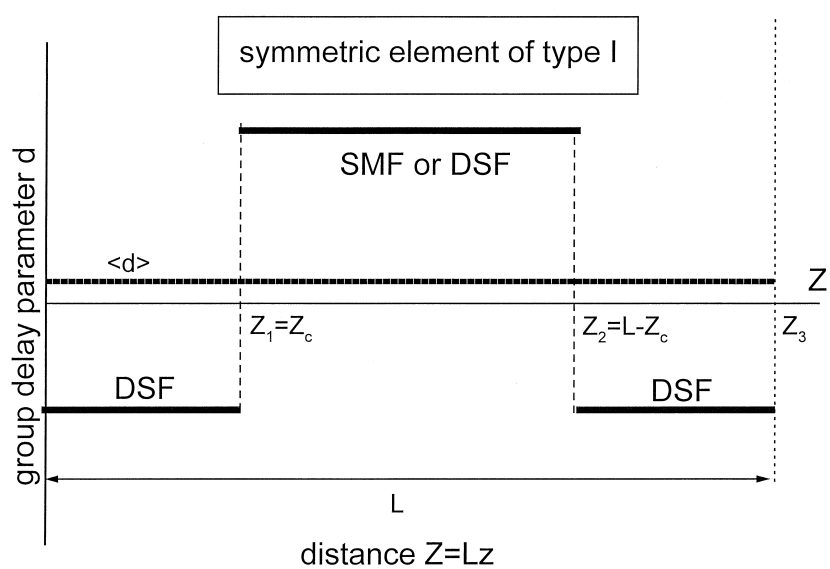

Fig. 1. Sketch of a symmetric element for dispersion compensation. The characteristic of type I is that the segments have consecutively negative, positive, and negative group delay parameters, respectively.

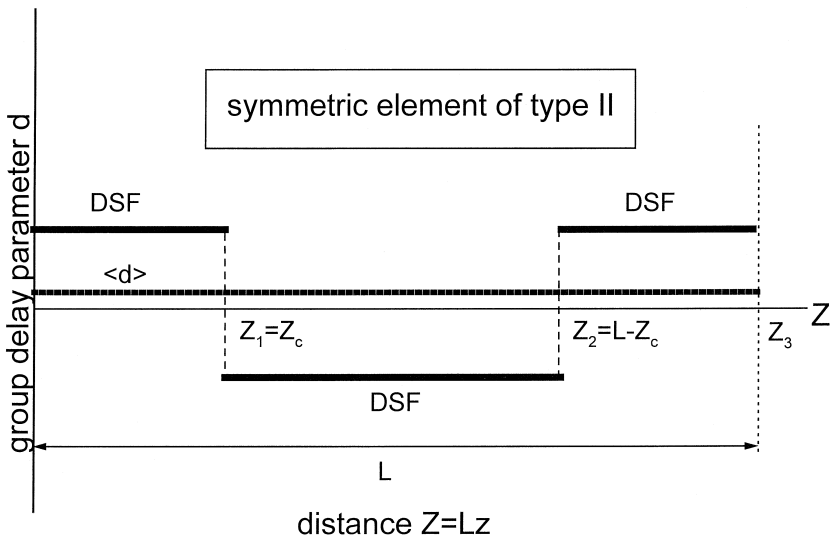

Fig. 2. Sketch of a symmetric element for dispersion compensation. The characteristic of type II is that the segments have consecutively positive, negative, and positive group delay parameters, respectively.

allows to increase the signal-to-noise ratio, which results in a substantial improvement of the system performance. An optical pulse propagating in an optical link with dispersion management acquires a chirp and experiences large-amplitude breathing oscillations of the pulse width. The energy of this dispersion-managed (DM) pulse is fixed by the system parameters (dispersion map, amplification distance, dispersion compensation period). An arbitrary RZ pulse launched into the system will emit radiation whose level can be rather high, which leads to significant degradation of the system performance. The input pulse chirp and energy should fit the corresponding chirp and energy, respectively, of the DM soliton for a specific dispersion map in order to diminish the shedding of radiation from the pulse into a dispersive pedestal [28,20,31,32,40,30].

In this paper we consider an (approximate) variational description for the optical pulse evolution in fiber links with varying dispersion [13,25–28]. One segment of the transmission line (including optical amplifiers with a small spacing between them) is called an element of the transmission line. Two examples are depicted in Fig. 1 and Fig. 2. An optical pulse propagating along a line (consisting of many elements) must be periodically reproduced at the output of each element. The transformation of the pulse after propagation in an element can be considered as the mapping of the input pulse into the output one. Therefore, for information transport we have to determine the fixed point of such a mapping. It will be shown that stable fixed points exist in properly designed modern transmission systems based on low dispersion fibers.

Additional parameters characterizing the influence of dispersion and nonlinearity are the dispersion length $Z_{\mathrm{dis}} \equiv t_0^2/\beta_2$ and the nonlinearity length $Z_{\mathrm{nl}} \equiv 1/(\sigma P_0)$, where σ is the coefficient of the Kerr nonlinearity. Furthermore, t_0 is the characteristic time, P_0 is the peak power, and β_2 is the local fiber chromatic dispersion. Obviously, we have an additional dispersion length corresponding to the residual (average) dispersion: $Z_{\mathrm{res}} \equiv t_0^2/|\langle \beta_2 \rangle|$. In the guiding-center theory $Z_{\mathrm{a}} \ll Z_{\mathrm{dis}} = Z_{\mathrm{nl}} = Z_{\mathrm{sol}}$. We consider the practical case $Z_{\mathrm{dis}} \ll Z_{\mathrm{nl}} \approx Z_{\mathrm{res}}$. In this limit one can treat nonlinearity and residual dispersion as small perturbations to the main effect of the varying high local dispersion. Consequently, the pulse dynamics can be described as linear with small deviations due to nonlinearity and residual dispersion.

The paper is organized as follows. In Section 2 we present the basic equations. The variational method to find appropriate solutions and optimized operational points is explained in Section 3. In Section 4 we show two basic arrangements for dispersion compensation, and typical parameter values are discussed. Analytical solutions for the piecewise constant dispersions are obtained in Section 5. From these expressions the fixed points of the mapping are obtained. In Section 6, the shape of the dispersion managed pulse is discussed in more detail. The paper is concluded by a short summary.

2. Basic equations

The evolution of optical pulses in fibers with damping and amplification can be described by a generalization of the cubic nonlinear Schrödinger equation. In dimensionless variables the master equation takes the form [29]

$$i\Psi_z + d(z)\Psi_{tt} + \frac{L}{Z_{\mathrm{nl}}}|\Psi|^2\Psi = iG(z)\Psi, \tag{1}$$

$$G(z) = L\left[-\gamma + r\sum_{k=1}^{N}\delta(z - z_k)\right]. \tag{2}$$

We use the following normalizations: The space coordinate Z is normalized by the length L of an element, i.e. $z = Z/L$ (see Figs. 1 and 2); time is measured in units of the input pulse width t_0; the envelope of the electric field $E = E(t,z)$ is normalized to the initial pulse power P_0 in the form $|E|^2 = P_0 t_0 |\Psi|^2$. Actually, we should note that there are different local dispersion lengths $Z_{\rm dis}^{(k)} = t_0^2/|\beta_2^{(k)}|$ since the dispersion is not constant (see Figs. 1 and 2). We also have to define a residual dispersion length $Z_{\rm res} = t_0^2/|\langle \beta_2 \rangle|$. Here β_2 is the group velocity dispersion that depends on z, and $\langle\ \rangle$ means averaging over the whole line. The coefficient γ describes fiber losses; r is the coefficient of amplification which should compensate the fiber losses over the (normalized) distance $z_{\rm a} = Z_{\rm a}/L$; finally $z_k = Z_k/L$ are the (normalized) locations of the amplifiers. From the dispersion relation we obtain the local group delay parameter

$$d(z) = -\frac{\beta_2(z)L}{2t_0^2}. \tag{3}$$

The amplification period could be different from the dispersion compensation period. Then the periodic amplification and the dispersion compensation can be handled as separate problems, provided the amplification distance is substantially different from the period of dispersion compensation [19].

It is convenient to transform Ψ to a new function A by taking out rapid oscillations of the amplitude due to periodic amplification:

$$\Psi = A(t,z)\exp\left[\int_0^z G(z')\,{\rm d}z'\right]. \tag{4}$$

Then the equation for A reads

$$iA_z + d(z)A_{tt} + c(z)|A|^2 A = 0, \tag{5}$$

where $c(z) \equiv c_0 \exp(2\int_0^z G(z')\,{\rm d}z')$ with

$$c_0 = P_0 L\sigma. \tag{6}$$

The coefficient $c(z)$ can be represented as a sum of rapidly varying and constant parts, i.e. $c(z) = \langle c(z)\rangle + \tilde{c}(z)$, where $\langle \tilde{c}(z)\rangle = 0$ and $\langle c(z)\rangle = c_0\langle \exp[2\int_0^z G(z')\,{\rm d}z']\rangle = c_0[1 - \exp(-2\gamma Z_{\rm a})]/(2\gamma Z_{\rm a})$. The average value is defined here as $\langle f\rangle = \int_0^1 f(z)\,{\rm d}z$. We write also $d(z)$ in the form $d(z) = \langle d(z)\rangle + \tilde{d}(z)$, where $\langle \tilde{d}(z)\rangle = 0$ and $\langle d(z)\rangle$ is a small contribution due to an average residual dispersion ($Z_{\rm dis}^{(k)}/Z_{\rm res} \ll 1$).

3. Variational approach

Eq. (5) can be rewritten in the Lagrangian form, with the action defined as

$$S = \int L\,{\rm d}t\,{\rm d}z = \int {\rm d}t\,{\rm d}z\left[\frac{i}{2}(AA_z^* - A^*A_z) + d(z)|A_t|^2 - \frac{c(z)}{2}|A|^4\right]. \tag{7}$$

To describe fast pulse-width oscillations let us choose a trial function in the form

$$A(z,t) = a(z)f[t/T(z)]\exp[i\lambda(z) + i\mu(z)t^2]. \tag{8}$$

The choice of this trial function is based on the following arguments. Any pulse is characterized by its amplitude a and width T. Furthermore, the phase variation should allow for frequency (or wavelength) variations and chirp via λ and μ, respectively. The form f of the pulse is still arbitrary, one possibility could be a Gaussian. We shall come back to this point in Section 6.

Inserting the trial function (8) into Eq. (7) we obtain a reduced variational problem with the averaged action

$$\langle S\rangle \equiv \int \langle L\rangle {\rm d}z, \tag{9}$$

where

$$\langle L\rangle(z) = a^2 T\int |f(s)|^2\,{\rm d}s\,\lambda_z + a^2T^3\int s^2|f(s)|^2\,{\rm d}s\,\mu_z + d(z)\left[a^2T^{-1}\int |f_s(s)|^2\,{\rm d}s + 4\mu^2a^2T^3\int s^2|f(s)|^2\,{\rm d}s\right]$$
$$- \frac{c(z)}{2}a^4T\int |f(s)|^4\,{\rm d}s. \tag{10}$$

One can derive equations describing the evolution of the parameters $\varphi(z) = a(z)$, $T(z)$, $\lambda(z)$, and $\mu(z)$ from the prescription (see e.g. Refs. [13,26–28,35])

$$\frac{\partial \langle L \rangle}{\partial \varphi} - \frac{\mathrm{d}}{\mathrm{d}z}\frac{\partial \langle L \rangle}{\partial \varphi_z} = 0; \quad \varphi(z) = \lambda(z), \mu(z), a(z), T(z).$$

The results are

$$a^2 T = \text{const} = 1, \tag{11}$$

$$\frac{\mathrm{d}T}{\mathrm{d}z} = 4d(z)T\mu, \tag{12}$$

$$\frac{\mathrm{d}\mu}{\mathrm{d}z} + 4d(z)\mu^2 = \left[\frac{d(z)C_1}{T^4} - \frac{c(z)C_2}{T^3}\right]. \tag{13}$$

Here,

$$C_1 = \frac{\int_{-\infty}^{+\infty} |f_x|^2 \,\mathrm{d}x}{\int_{-\infty}^{+\infty} x^2 |f|^2 \,\mathrm{d}x}, \tag{14}$$

and

$$C_2 = \frac{\int_{-\infty}^{+\infty} |f|^4 \,\mathrm{d}x}{4\int_{-\infty}^{+\infty} x^2 |f|^2 \,\mathrm{d}x}. \tag{15}$$

In the dimensional form, the pulse energy is given by

$$\mathscr{E} = P_0 t_0 \int |f(x)|^2 \,\mathrm{d}x = P_0 t_0 \,\rho C_2 C_1^{-3/4}. \tag{16}$$

For a specific choice of a trial function f one can find the dependence of the soliton energy on the parameters of the system and on the input pulse. For instance, for $Q(x) = A\exp(-0.5x^2/x_0^2)$ it is easy to find that $C_1 = 1/x_0^4$ and $C_2 = A^2/(2x_0^2\sqrt{2})$. In most examples considered in this paper we approximate the shape of the input signal by a Gaussian pulse. The pulse width T_{FWHM} (full width at half maximum) is then found as $T_{\mathrm{FWHM}} = 1.665\, C_1^{-1/4}\, t_0$. It should be noted that the energy $\mathscr{E}$ of the asymptotic pulse is proportional to C_2, i.e.

$$\mathscr{E} = P_0 t_0 2\sqrt{2\pi}\, C_2 C_1^{-3/4}. \tag{17}$$

We can derive the same expression for a sech-shaped soliton. In this case, $T_{\mathrm{FWHM}} = 1.763\, C_1^{-1/4}\, t_0 \sqrt{2/\pi}$. In general, for an arbitrary pulse shape we have $T_{\mathrm{FWHM}} = \alpha\, C_1^{-1/4}\, t_0$, where α is determined by the pulse form and the energy is given by Eq. (16).

Introducing $M = \mu T$ we can obtain from Eqs. (12) and (13)

$$\frac{\mathrm{d}M}{\mathrm{d}z} = \frac{d(z)C_1}{T^3} - \frac{c(z)C_2}{T^2}. \tag{18}$$

Eqs. (12) and (18) have been first derived (in the context of dispersion-manged soliton transmission) in Ref. [13]. These equations are fundamental for the description of the dynamics of the energy-bearing part of the dispersion-managed soliton. To describe periodic breathing pulses propagating along the cascaded line, solutions of these equations must satisfy two evident conditions of periodicity: $T(1) = T(0)$ and $M(1) = M(0)$, or applying this to Eqs. (12) and (18),

$$\langle d(z)M \rangle = 0, \tag{19}$$

and

$$\left\langle \frac{d(z)C_1}{T^3} \right\rangle = \left\langle \frac{c(z)C_2}{T^2} \right\rangle. \tag{20}$$

Here the angular brackets mean averaging over the compensation period. These conditions allow to determine the power enhancement and to link the width as well as the chirp of a dispersion-managed soliton at some points with the system

parameters. Additionally, taking into account that $c(z)$ is strictly positive, we obtain the necessary condition for the existence of a dispersion-managed soliton as $\langle d(z)/T^3\rangle > 0$. Simple manipulations of Eqs. (12) and (18) give also that

$$\langle d(z)/T^2\rangle = \langle c(z)C_2/\left(T\left[1+4M^2T^2\right]\right)\rangle > 0,$$

which is a necessary condition for the existence of the periodic solution of Eqs. (12) and (18). As it will be shown below, this condition will appear also when considering the soliton form. It can be satisfied even if the average dispersion is zero or normal.

Following Ref. [41] we now present briefly a simple physical explanation for the fact that DM solitons can propagate at zero or normal average dispersion. Qualitatively, a possibility to balance nonlinear and dispersive effects at zero or normal dispersion results from the large variation of the soliton width during one compensation period, and the self-similar structure of the DM soliton given by Eq. (8). A phase shift generated by the dispersion, estimated as $\Delta\Phi = -\beta_2/[2T^2] \sim D/T^2$, is proportional to the dispersion D and is inversely proportional to the square of the pulse width. In the case of a constant pulse width, this condition determines the power of the fundamental soliton since one should have a balance with the corresponding nonlinear phase shift. In the case of varying widths (as for DM solitons) the balance is achieved on average. It can be easily shown that the dispersion-induced phase shift, averaged over one period $\langle D(z)/T^2(z)\rangle$ can be positive even if $\langle D(z)\rangle$ is zero or negative (normal dispersion). Thus, a balance can be achieved if $\langle D(z)/T^2(z)\rangle$ is positive even at zero or normal average dispersion. Equating the averaged phase shifts due to dispersion $\langle\Delta\Phi_D\rangle = -\langle\beta_2(z)/[2T^2(z)]\rangle$ and nonlinearity $\langle\Delta\Phi_{NL}\rangle = \sigma\langle c(z)/T(z)]\rangle$, one can obtain an estimation of the peak power enhancement. Of course, this is only a rough estimation, because there is an additional phase shift due to pulse chirping that should be taken into account. In terms of the approach developed above, the total phase shift can be presented as

$$\frac{\mathrm{d}(TM)}{\mathrm{d}z} = 4dM^2 + \frac{dC_1}{T^2} - \frac{cC_2}{T}. \tag{21}$$

Here, TM is proportional to the rapidly oscillating part of the soliton phase in accordance with Eq. (8). Recovering the soliton phase (except linear growth) leads to the condition

$$\langle d(z)\left[4M^2 + C_1/T^2\right]\rangle = \langle c(z)/T(z)\rangle C_2 > 0.$$

The physical interpretation of this condition is obvious: The construction $4M^2 + C_1/T^2 = \Omega^2(z)$ is nothing else that the square of the varying spectral bandwidth Ω of a chirped pulse. The total phase shift due to pulse chirping, dispersion and nonlinearity should be zero (balanced) on average for true periodic propagation. It can be easily found that the requirement of anomalous average dispersion $\langle D(z)\rangle > 0$ that provides the existence of the traditional NLSE soliton is replaced for the DM soliton by the condition $D_{\mathrm{eff}} = \langle D(z)\Omega^2\rangle > 0$ that can be satisfied at zero and even normal-averaged dispersion. Note that soliton far-field tails (having small amplitudes) are not self-similar [20], and this provides stability against tunneling [38]. The latter occurs for self-similar solutions due to the non-trapping parabolic potential resulting from the pulse chirping [38,36].

In the following, we consider $d(z)$ as a result from combining pieces with positive and negative constant values (see Figs. 1 and 2). This situation is identical to the dispersion compensation schemes used in practice. Then, from Eqs. (12) and (18) we can obtain a single equation for the function T which is valid in the regions of constant d,

$$\frac{\mathrm{d}^2T}{\mathrm{d}z^2} = 4d(z)\left[\frac{C_1d(z)}{T^3} - \frac{c(z)C_2}{T^2}\right]. \tag{22}$$

At the jumps of the dispersion coefficient we assume continuity of T and M. Initial conditions to Eq. (22) are

$$[T]_{z=0} = 1, \quad \left[\frac{\mathrm{d}T}{\mathrm{d}z}\right]_{z=0} = 4M_0d(0). \tag{23}$$

Note that the Gaussian approximation for the pulse shape is not a principal limitation of the method. Any localized pulse can be considered in a similar manner, using the above link between pulse shape f and coefficients C_1, C_2. It can be easily shown that the fast dynamics of the asymptotic dispersion-managed soliton formed in the line with dispersion compensation is always described by the system of equations (12) and (18) with C_1 and C_2 recalculated from the pulse shape through Eqs. (14) and (15). Thus, Eqs. (12) and (18) give a very effective and clear prescription to optimize dispersion-managed fiber transmission systems.

For any further calculations we have to specify more detailed structures for possible dispersion compensations, i.e. the function $d(z)$. This will be done in the next section.

4. Dispersion compensation arrangements

As the basic application in this paper we will consider symmetric dispersion maps, as suggested in Refs. [18,19]. We also restrict ourselves to the non-fluctuating and lossless case $c(z) = c_0 = 1$. Of course, losses are always present in real fibers. However, if the period of the dispersion map is different from the amplification period, the model can be reduced to the lossless case. For instance, if the dispersion compensation period is much larger than the amplification period (as it is assumed here), one can average over the fast oscillations between two consecutive amplifiers. Then a lossless model with varying dispersion will be a good approximation for the slow pulse dynamics in the real system.

We distinguish between two types of symmetric elements. Symmetric elements of the first kind (see Fig. 1) consisting of a compensating fiber with a group delay parameter $d_2 > 0$ and length $L - 2Z_c$, which is surrounded by two pieces of fiber with the group delay parameter $d_1 < 0$ and length Z_c. And this configuration is repeated periodically. Practically, in this design we can use DSF with normal dispersion as a transmission fiber, and SMF as a compensating fiber in the center. Alternatively, the element can be built from pieces of DSF with different dispersions. Definitely, these elements can be used in long-haul transmission systems in which the dispersion compensation period is much larger than the amplification distance. Averaging over amplification leads effectively to a lossless model. Though, these two types of compensation elements can be obtained from each other by appropriate shifts, we consider them separately. The difference is not in the order of the transmission and compensation fibers, but mostly in the symmetry of the map. In the map of the first type (with SMF in the center) it will be shown that the map strength is bounded from above and in the second configuration (symmetrical pieces of DSF) the map strength is not limited.

The strength of the element can be characterized by [18,19,25]

$$K = \left| \frac{2Z_c \tilde{\beta}_2^{(1)} - \tilde{\beta}_2^{(2)}(L - 2Z_c)}{2t_0^2} \right|. \tag{24}$$

Define $Z_c = z_c L$, then $2\tilde{d}_1 z_c + \tilde{d}_2(1 - 2z_c) = 0$ yields

$$Z_c = \frac{\tilde{d}_2}{2\left(\tilde{d}_2 - \tilde{d}_1\right)} L, \tag{25}$$

and the strength parameter becomes

$$K = \left| \frac{2\tilde{d}_1 \tilde{d}_2}{\tilde{d}_2 - \tilde{d}_1} \right| = \frac{2\tilde{d}_1 \tilde{d}_2}{\tilde{d}_1 - \tilde{d}_2}. \tag{26}$$

Note that our definition of the map strength is a bit different from that introduced in Refs. [18,19]. In our definition a fixed time parameter t_0 is used whereas in Refs. [18,19] T_{FWHM} was used. Let us consider an example in which $\tilde{d}_2$ is fixed. For $L = 120$ km, $\tilde{\beta}_2^{(2)} = -20$ ps^2/km, $t_0 = 10$ ps, one obtains $\tilde{d}_2 = 12$. We add the residual dispersion $\langle d \rangle$ everywhere, and we can write

$$d(z) = \begin{cases} -12K/(24 - K) + \langle d \rangle & \text{for } 0 \le z < z_c, \\ 12 + \langle d \rangle & \text{for } z_c < z < 1 - z_c, \\ -12K/(24 - K) + \langle d \rangle & \text{for } 1 - z_c < z < 1, \end{cases} \tag{27}$$

since

$$\tilde{d}_1 = -\frac{\tilde{d}_2 K}{2\tilde{d}_2 - K}, \quad \tilde{d}_2 = \frac{\tilde{d}_1 K}{2\tilde{d}_1 + K}. \tag{28}$$

As mentioned before, we use the initial conditions $T(0) = 1$ and $M(0) = M_0$. The parameter $K = -2\tilde{d}_1\tilde{d}_2/(\tilde{d}_2 - \tilde{d}_1)$ formally varies from 0 to 24 in the case at hand. The length of the first fiber piece is found as $Z_c = LK/(-4\tilde{d}_1)$ km. In the forthcoming discussion we shall choose two versions. In the first one, we assume a typical value for the residual dispersion, e.g. $\langle d \rangle = 0.2$, and consider K as a variable. In the second version K is a fixed parameter and we vary $\langle d \rangle$.

Another type of symmetric map is constructed as follows (see Fig. 2): First, a fiber with anomalous dispersion ($d_1 > 0$; DSF or SMF), then a middle fiber, with normal dispersion ($d_2 < 0$; DSF or DCF), and finally a third piece, identical to the first one. It should be pointed out that in this case the soliton transmission is possible although the line could be built mostly from the fiber with normal dispersion. The only requirement is that the path-average dispersion is anomalous.

Introducing the strength parameter K as $K = 2\tilde{d}_1\tilde{d}_2/(\tilde{d}_2 - \tilde{d}_1)$ for the general case, we obtain for $\tilde{d}_1 > 0$ and $\tilde{d}_2 < 0$

$$\tilde{d}_1 = \frac{\tilde{d}_2 K}{2\tilde{d}_2 + K}, \quad \tilde{d}_2 = \frac{\tilde{d}_1 K}{-2\tilde{d}_1 + K}, \quad Z_c = \frac{K}{4\tilde{d}_1} L. \tag{29}$$

In summary, we have the group delay parameter

$$d(z) = \begin{cases} \tilde{d}_1 + \langle d \rangle & \text{for } 0 \le z < z_c, \\ \tilde{d}_1 K/\left(-2\tilde{d}_1 + K\right) + \langle d \rangle & \text{for } z_c < z < 1 - z_c, \\ \tilde{d}_1 + \langle d \rangle & \text{for } 1 - z_c < z < 1. \end{cases} \tag{30}$$

Typical parameters for such a map can be found in Ref. [18]. A quite interesting situation occurs if one considers a line constructed from DSF pieces of equal lengths and opposite dispersions with $\tilde{d}_1 = -\tilde{d}_2 = d_0$. It yields $K = d_0$. We shall investigate this case for the parameters $L = 200$ km, $t_0 = 10$ ps, $\langle \beta_2 \rangle = -0.15$ ps^2/km, $\tilde{\beta}_2^{(1)} = -5$ ps^2/km, and $\tilde{\beta}_2^{(2)} = 5$ ps^2/km leading to $\tilde{d}_1 = 5$ and $\langle d \rangle = 0.15$.

5. Analytical solutions for piecewise constant dispersion

There are no major difficulties for solving Eq. (5) in the (effectively) lossless case $c(z) = \text{const}$ and for piecewise constant group delay parameters $d(z)$ as prescribed in the previous section.

In the limit L, $Z_{\text{dis}} \ll Z_{\text{nl}}$, one may treat the nonlinearity as a perturbation and assume $T(z) \approx T_{\text{lin}}(z)$ as well as $M(z) \approx M_{\text{lin}}(z)$. We make this approximation first in order to get a simple insight into the expected behavior. Then, in the lowest order, fast oscillations of the pulse amplitude and width are given by a solution of the linear problem

$$\frac{\mathrm{d}^2 T_{\text{lin}}}{\mathrm{d}z^2} = \frac{4C_1[d(z)]^2}{T_{\text{lin}}^3}, \tag{31}$$

which originates from

$$\frac{\mathrm{d}T_{\text{lin}}}{\mathrm{d}z} = 4d(z) M_{\text{lin}}, \tag{32}$$

$$\frac{\mathrm{d}M_{\text{lin}}}{\mathrm{d}z} = \frac{d(z) C_1}{T_{\text{lin}}^3}, \tag{33}$$

in the regions where $d(z) = \text{const}$. The procedure to solve these equations is as follows. We start at $z = 0$ where $T_{\text{lin}}(0) = 1$ and $M_{\text{lin}}(0) = M_0$ are given. That means that

$$\frac{\mathrm{d}T_{\text{lin}}}{\mathrm{d}z}(z = 0) = 4d(0) M_0$$

is also known. Now we assume constant dispersions in the regions $0 \le z \le z_1^-$, $z_1^+ \le z \le z_2^-$, $z_2^+ \le z \le z_3^-$, and so on. Here we have introduced the notations $z_\nu^- = (z_\nu - \epsilon)$ and $z_\nu^+ = (z_\nu + \epsilon)$ in the limits $\epsilon \to +0$. Having a starting point z_n^+, e.g. for $n = 0$: $z_0^+ = 0$, we can easily integrate from z_n^+ to z_{n+1}^- since we assume that in that region $d(z) = \tilde{d}_n + \langle d \rangle$ is constant. In the transition from z_n^- to z_n^+ T and M are continuous:

$$T(z_n^-) = T(z_n^+) \equiv T(z_n), \quad M(z_n^-) = M(z_n^+) \equiv M(z_n), \tag{34}$$

whereas in the dispersion and in the derivatives we have jumps:

$$d(z_n^-) \ne d(z_n^+), \quad \frac{\mathrm{d}T}{\mathrm{d}z}(z_n^-) \ne \frac{\mathrm{d}T}{\mathrm{d}z}(z_n^+), \quad \frac{\mathrm{d}M}{\mathrm{d}z}(z_n^-) \ne \frac{\mathrm{d}M}{\mathrm{d}z}(z_n^+). \tag{35}$$

For example, from Eq. (32) we find

$$\frac{\mathrm{d}T}{\mathrm{d}z}(z_{n+1}^+) = \frac{\tilde{d}_{n+1} + \langle d \rangle}{\tilde{d}_n + \langle d \rangle} \frac{\mathrm{d}T}{\mathrm{d}z}(z_{n+1}^-). \tag{36}$$

These relations are written for the general case; of course, they can be also used in the linear situation.

Let us now integrate Eq. (31) in the region $z_n^+ \le z \le z_{n+1}^-$. We obtain

$$T_{\mathrm{lin}}(z) = \sqrt{\frac{b_n}{a_n} + \frac{1}{a_n}\left[\sqrt{a_n T_{\mathrm{lin}}^2(z_n) - b_n} \pm \frac{a_n}{2}(z - z_n)\right]^2}, \quad z_n^+ \le z \le z_{n+1}^-, \tag{37}$$

where

$$a_n = \frac{16C_1\left(\tilde{d}_n + \langle d\rangle\right)^2}{T_{\mathrm{lin}}^2(z_n)} + 4\left[\frac{\mathrm{d}T_{\mathrm{lin}}}{\mathrm{d}z}(z_n^+)\right]^2 \tag{38}$$

and

$$b_n = 16C_1\left(\tilde{d}_n + \langle d\rangle\right)^2. \tag{39}$$

Alternatively, we can present the linear solution in terms of $T_{\mathrm{lin}}(z_n)$ and $M_{\mathrm{lin}}(z_n)$, namely

$$T_{\mathrm{lin}}^2(z) = T_{\mathrm{lin}}^2(z_n)\frac{C_1 + 4\left[M_{\mathrm{lin}}(z_n)T_{\mathrm{lin}}(z_n) \pm d_n(z - z_n)\left(C_1 + 4M_{\mathrm{lin}}^2(z_n)T_{\mathrm{lin}}^2(z_n)\right)/T_{\mathrm{lin}}^2(z_n)\right)\right]^2}{C_1 + 4M_{\mathrm{lin}}^2(z_n)T_{\mathrm{lin}}^2(z_n)}. \tag{40}$$

Obviously, we have

$$\frac{\mathrm{d}T_{\mathrm{lin}}}{\mathrm{d}z}(z) = \pm\frac{1}{2}\sqrt{a_n - \frac{b_n}{\left[T(z)\right]^2}} \quad \text{for } z_n^+ \le z \le z_{n+1}^-. \tag{41}$$

We have to distinguish between the cases of positive and negative derivatives of T. The symbol $\pm$ takes care of the signs of the derivatives.

Now we are ready to iterate

$$T_{\mathrm{lin}}(z_n^+) \equiv T_{\mathrm{lin}}(z_n) \Rightarrow T_{\mathrm{lin}}(z_{n+1}^+) \equiv T_{\mathrm{lin}}(z_{n+1}), \tag{42}$$

$$\frac{\mathrm{d}T}{\mathrm{d}z}(z_n^+) \Rightarrow \frac{\mathrm{d}T}{\mathrm{d}z}(z_{n+1}^-) \Rightarrow \frac{\mathrm{d}T}{\mathrm{d}z}(z_{n+1}^+). \tag{43}$$

In detail it reads

$$a_n = \frac{16C_1\left(\tilde{d}_n + \langle d\rangle\right)^2}{T_{\mathrm{lin}}^2(z_n)} + 4\left[\frac{\mathrm{d}T_{\mathrm{lin}}}{\mathrm{d}z}(z_n^+)\right]^2, \tag{44}$$

$$b_n = 16C_1\left(\tilde{d}_n + \langle d\rangle\right)^2, \tag{45}$$

$$T_{\mathrm{lin}}(z_{n+1}) = \sqrt{\frac{b_n}{a_n} + \frac{1}{a_n}\left[\sqrt{a_n T_{\mathrm{lin}}^2(z_n) - b_n} \pm \frac{a_n}{2}(z_{n+1} - z_n)\right]^2}, \tag{46}$$

and

$$\frac{\mathrm{d}T_{\mathrm{lin}}}{\mathrm{d}z}(z_{n+1}^+) = \frac{\tilde{d}_{n+1} + \langle d\rangle}{\tilde{d}_n + \langle d\rangle}\left\{\pm\frac{1}{2}\sqrt{a_n - \frac{b_n}{\left[T_{\mathrm{lin}}(z_{n+1})\right]^2}}\right\}. \tag{47}$$

We abbreviate this iteration step by

$$\left\{T_{\mathrm{lin}}, \frac{\mathrm{d}T_{\mathrm{lin}}}{\mathrm{d}z}\right\}_{n+1} = \mathscr{M}_{\mathrm{lin}}^{(1)}\left\{T_{\mathrm{lin}}, \frac{\mathrm{d}T_{\mathrm{lin}}}{\mathrm{d}z}\right\}_n. \tag{48}$$

This is a clear prescription which can be used straightforwardly for the mapping along a given line. For the dispersion compensating elements discussed in the previous section, it is appropriate to perform three iterations in order to relate the output of an element to the input. We can write

$$\left\{T_{\mathrm{lin}}, \frac{\mathrm{d}T_{\mathrm{lin}}}{\mathrm{d}z}\right\}_3 = \mathscr{M}_{\mathrm{lin}}^{(1)}\mathscr{M}_{\mathrm{lin}}^{(1)}\mathscr{M}_{\mathrm{lin}}^{(1)}\left\{T_{\mathrm{lin}}, \frac{\mathrm{d}T_{\mathrm{lin}}}{\mathrm{d}z}\right\}_0 \equiv \mathscr{M}_{\mathrm{lin}}^{(3)}\left\{T_{\mathrm{lin}}, \frac{\mathrm{d}T_{\mathrm{lin}}}{\mathrm{d}z}\right\}_0. \tag{49}$$

Of course the fixed points of the mapping $\mathscr{M}_{\mathrm{lin}}^{(3)}$ are of interest. Before discussing these interesting solutions and their consequences for technical applications, let us extend the situation to the nonlinear case.

Nonlinear effects come into play on a large scale compared to L, namely at distances proportional to $Z_{\rm nl}$. Analytical solutions for constant dispersion were first obtained in Ref. [35] and used recently in the context of dispersion management in Refs. [33,34]. Instead of Eq. (31) now we have to integrate Eq. (22), i.e.

$$\frac{\mathrm{d}^2T}{\mathrm{d}z^2} = 4d(z)\left[\frac{C_1 d(z)}{T^3} - \frac{c(z)C_2}{T^2}\right]. \tag{50}$$

A calculation similar to the one above leads now to

$$F_n[T(z)] = F_n[T(z_n)] \pm \frac{\tilde{a}_n}{2}(z - z_n), \quad z_n^+ \le z \le z_{n+1}^-. \tag{51}$$

Here

$$F_n[T(z)] \equiv \sqrt{\tilde{a}_n T^2(z) + \tilde{c}_n T(z) - \tilde{b}_n} - \frac{\tilde{c}_n}{2}\frac{1}{\sqrt{\tilde{a}_n}}\ln\left[2\sqrt{\tilde{a}_n}\sqrt{\tilde{a}_n T^2(z) + \tilde{c}_n T(z) - \tilde{b}_n} + 2\tilde{a}_n T(z) + \tilde{c}_n\right], \tag{52}$$

$$\tilde{a}_n = \frac{16C_1\left(\tilde{d}_n + \langle d\rangle\right)^2}{T^2(z_n)} + 4\left[\frac{\mathrm{d}T}{\mathrm{d}z}(z_n^+)\right]^2 - \frac{\tilde{c}_n}{T(z_n)}, \tag{53}$$

$$\tilde{b}_n = b_n, \tag{54}$$

$$\tilde{c}_n = 32c_0C_2\left(\tilde{d}_n + \langle d\rangle\right). \tag{55}$$

Clearly, for $\tilde{c}_n \to 0$ we recover the linear result (31). However, we cannot invert F_n, i.e. we cannot explicitly solve for $T(z)$. On the other hand, once we have determined $T(z_{n+1}^-) \equiv T(z_{n+1})$ from Eq. (51), i.e.

$$F_n[T(z_{n+1})] = F_n[T(z_n)] \pm \frac{\tilde{a}_n}{2}(z_{n+1} - z_n), \tag{56}$$

we can find $\mathrm{d}T(z_{n+1}^-)/\mathrm{d}z$ from

$$\frac{\mathrm{d}T}{\mathrm{d}z}(z_{n+1}^-) = \pm\frac{1}{2}\sqrt{\tilde{a}_n + \frac{\tilde{c}_n}{T(z_{n+1})} - \frac{\tilde{b}_n}{\left[T(z_{n+1})\right]^2}}\ . \tag{57}$$

Finally, from Eq. (36), i.e.

$$\frac{\mathrm{d}T}{\mathrm{d}z}(z_{n+1}^+) = \frac{\tilde{d}_{n+1} + \langle d\rangle}{\tilde{d}_n + \langle d\rangle}\frac{\mathrm{d}T}{\mathrm{d}z}(z_{n+1}^-),$$

we obtain the jump in the derivative. This completes the outline for the map in the nonlinear case. (All the other steps are similar to those described previously for the linear map.)

Finally, let us make the assumption that residual dispersion and nonlinearity only slightly affect the pulse shape T and chirp parameter M over one compensation period. As mentioned before, such condition is practical and is satisfied in systems with moderate or strong dispersion management. This assumption allows to obtain explicitly the next correction to the linear solution $T_{\rm lin}$ using $c_{\tilde{n}}$ and $\langle d\rangle$ as small parameters. Let us rewrite Eq. (51) in the form

$$\tilde{a}_n T^2(z) + \tilde{c}_n T(z) - \tilde{b}_n = \left[\pm\frac{\tilde{a}_n}{2}(z - z_n) + F_n[T(z_n)] + \tilde{c}_n R_1(z)\right]^2, \tag{58}$$

where

$$R_1(z) = \frac{1}{2\sqrt{\tilde{a}_n}}\ln\left[2\sqrt{\tilde{a}_n}\sqrt{\tilde{a}_n T^2(z) + \tilde{c}_n T(z) - \tilde{b}_n} + 2\tilde{a}_n T(z) + \tilde{c}_n\right]. \tag{59}$$

Now we expand the function T and all coefficients using $\tilde{c}_n$ and $\langle d\rangle$ as small parameters. This yields

$$T(z) = T_{\rm lin}(z) + T_1(z) + \ldots \tag{60}$$

$$M(z) = M_{\rm lin}(z) + M_1(z) + \ldots \tag{61}$$

$$\tilde{a}_n = A_n + \delta a_n = \frac{16C_1\tilde{d}_n^2}{T_{\rm lin}^2(z_n)} + 64\tilde{d}_n^2 M_{\rm lin}^2(z) + \frac{32C_1\tilde{d}_n\langle d\rangle}{T_{\rm lin}^2(z_n)} - \frac{32C_1\tilde{d}_n^2 T_1(z_n)}{T_{\rm lin}^3(z_n)} + 128\tilde{d}_n\langle d\rangle M_{\rm lin}^2(z_n) + 128\tilde{d}_n^2 M_{\rm lin}(z_n)M_1(z_n) - \frac{\tilde{c}_n}{T_{\rm lin}(z_n)}, \tag{62}$$

$$\tilde{b}_n = B_n + \delta b_n = 16C_1\tilde{d}_n^2 + 32C_1\tilde{d}_n\langle d\rangle, \tag{63}$$

$$F_n[T(z_n)] = F_n^{(0)}[T(z_n)] + \delta F_n[T(z_n)], \tag{64}$$

Straightforward algebra gives

$$2A_nT_{\rm lin}(z)T_1(z) = \delta b_n - T_{\rm lin}^2(z)\delta a_n - \tilde{c}_nT_{\rm lin}(z) + 2\left[\pm\frac{A_n}{2}(z-z_n) + F_n^{(0)}\right] \times\left[\pm\frac{\delta a_n}{2}(z-z_n) + \delta F_n[T(z_n)] + \tilde{c}_nR_1(z)\right]. \tag{65}$$

The latter expression presents a small variation of T along the compensation element due to cumulative effects of residual dispersion and nonlinearity. An explicit expansion of this result gives

$$2A_nT_{\rm lin}(z)T_1(z) = \delta b_n - \delta a_nT_{\rm lin}^2(z) - \tilde{c}_nT_{\rm lin}(z) + 2\left[\pm\frac{A_n}{2}(z-z_n) + \sqrt{A_nT_{\rm lin}^2(z_n) - B_n}\right] \times\left[\pm\frac{\delta a_n}{2}(z-z_n) + \frac{2A_nT_{\rm lin}(z_n)T_1(z_n) + \delta a_nT_{\rm lin}^2(z_n) + \tilde{c}_nT_{\rm lin}(z_n) - \delta b_n}{2\sqrt{A_nT_{\rm lin}^2(z_n) - b_n}} + \frac{\tilde{c}_n}{2\sqrt{A_n}}\ln\left(\frac{\sqrt{A_nT_{\rm lin}^2(z) - B_n} + \sqrt{A_n}\,T_{\rm lin}(z)}{\sqrt{A_nT_{\rm lin}^2(z_n) - B_n} + \sqrt{A_n}\,T_{\rm lin}(z_n)}\right)\right].$$

At the points where $M(z) = 0$ (chirp-free points), i.e. $\sqrt{\tilde{a}_nT^2(z) + \tilde{c}_nT(z) - \tilde{b}_n} = 0$ we obtain

$$F_n^{(0)} = 0, \quad \delta F_n[T(z_n)] = -\frac{\tilde{c}_n}{2\sqrt{A_n}}\ln(2A_nT_{\rm lin}(z_n)).$$

The analogous form for the first correction of $M(z)$ is

$$M_1(z) = \pm\left(-\frac{\langle d\rangle}{8\tilde{d}_n^2}\sqrt{A_n - \frac{B_n}{T_{\rm lin}^2(z)}} + \frac{1}{16\tilde{d}_n}\frac{\delta a_n + \tilde{c}_n/T_{\rm lin}(z) - \delta b_n/T_{\rm lin}^2(z) + 2B_nT_1(z)/T_{\rm lin}^3(z)}{\sqrt{A_n - B_n/T_{\rm lin}^2(z)}}\right).$$

As an example of the analytical treatment of piecewise constant dispersion and the iteration using this first order perturbation theory we consider the special case of a symmetric type II element with $K = \tilde{d}_1 > 0$ and $\tilde{d}_2 = -\tilde{d}_1$ for $z \in [0,1]$. For convenience, in what follows we denote $\tilde{d}_1 = \tilde{d}$. Evaluation of the zero-order terms leads to

$$T := T_{\rm lin}\left(\tfrac{1}{4}\right) = \sqrt{1 + C_1\tilde{d}^2/4} = T_{\rm lin}\left(\tfrac{3}{4}\right), \quad T_{\rm lin}\left(\tfrac{1}{2}\right) = T_{\rm lin}(0) = T_{\rm lin}(1) = 1,$$

$$M_{\rm lin}\left(\tfrac{1}{4}\right) = \frac{C_1\tilde{d}/4}{\sqrt{1 + \frac{C_1\tilde{d}^2}{4}}} = -M_{\rm lin}\left(\tfrac{3}{4}\right), \quad M_{\rm lin}(0) = M_{\rm lin}\left(\tfrac{1}{2}\right) = M_{\rm lin}(1) = 0,$$

$$A := A_1 = A_2 = B_1 = B_2 = 16C_1\tilde{d}^2.$$

For the first order perturbation in the interval $\left[0, \tfrac{1}{4}\right]$ we obtain

$$2ATT_1\left(\tfrac{1}{4}\right) = \delta b_1 - \delta a_1T^2 - \tilde{c}_1T + \frac{A\delta a_1}{32} + \frac{\tilde{c}_1A}{8\sqrt{A}}\ln\left(\frac{\sqrt{A}}{8} + T\right).$$

To simplify the expressions, in the next step [$T_1(\frac{1}{4})$ and $M_1(\frac{1}{4})$ occur in the formulas for δa_2] we make use of the following relation,

$$\delta a_2 = -\delta a_1 + 2\tilde{c}_1\left(\frac{1}{T} - 1\right).$$

Considering the solutions in the interval $\left[\frac{1}{4},\frac{1}{2}\right]$ leads to

$$T_1(\tfrac{1}{2}) = \frac{\tilde{c}_1}{A}\left(1 - \frac{1}{T}\right). \tag{66}$$

The next step for the region $\left[\frac{1}{2},\frac{3}{4}\right]$ is similar to that in the interval $\left[0,\frac{1}{4}\right]$, hence

$$2ATT_1(\tfrac{3}{4}) = \delta b_2 - \delta a_2 T^2 - \tilde{c}_2 T + \frac{A\delta a_2}{32} + \frac{\tilde{c}_2 A}{8\sqrt{A}}\ln\left(\frac{\sqrt{A}}{8} + T\right).$$

Equating now $T_1(\frac{1}{4}) = T_1(\frac{3}{4})$ for a symmetric solution yields the dependence of the energy (proportional to C_2) on other parameters in first order perturbation theory:

$$c_0 C_2 = \frac{C_1\langle d\rangle}{2/\sqrt{1 + C_1\tilde{d}^2/4} - \left(2/\sqrt{C_1}\,\tilde{d}\right)\ln\left(\frac{1}{2}\sqrt{C_1}\,\tilde{d} + \sqrt{1 + C_1\tilde{d}^2/4}\right)}. \tag{67}$$

In the real-world variables this expression takes the form

$$\mathscr{E} = -\frac{\alpha\rho\langle\beta_2\rangle}{2\sigma T_{\mathrm{FWHM}}}\left(\frac{2}{\sqrt{1+x^2}} - \frac{\ln\left[x + \sqrt{1+x^2}\right]}{x}\right)^{-1}, \quad x = \frac{\Delta\beta L\alpha^2}{8T_{\mathrm{FWHM}}^2}. \tag{68}$$

We have used here the scaling parameters α and ρ introduced above to describe the arbitrary soliton shape. $\Delta\beta$ is the difference between dispersion of two pieces of fibers used in the map. This formula gives an analytical description of the soliton energy enhancement in transmission systems with dispersion management, first observed in Ref. [18]. More precisely, we used the only assumption that the residual dispersion and the nonlinearity act as small perturbations of the linear pulse oscillations over one compensation period. If the local dispersion is the main effect and the optical pulse behaves (during one compensation period) almost linearly, this perturbation works very well as it will be shown in the following numerical illustrations. As a matter of fact, this is the limit opposite to the case of a weak dispersion management for which an analytical description is also possible [30]. Of course, the perturbative approach breaks down if the pulse power (proportional to C_2) becomes not small (for instance, with further increasing of d or near the point x_{cr} at which the denominator is zero).

We now present the predictions based on these maps. In general, we are interested in the periodic solutions (with periodicity length L, i.e. after passing through an element). They correspond to the fixed points of the map $\mathscr{M}^{(3)}$. Before presenting the general conditions for periodic solutions, let us start with a specific example. We choose a symmetric element of type I and take the parameters $K = 3$, $\langle d\rangle = 0.2$, $C_1 = 0.5$, $C_2 \approx 0.2563$ which, indeed, belong to a fixed point. In Fig. 3, $T(z)$ and $M(z)$ are shown, respectively. As we can recognize, in each element, a pulse undergoes periodic broadening and recompression. A similar situation occurs for the chirp. The pulse can pass through many elements without a significant changes of its form at the output. The comparison of the variational approach (squares for T and crosses for M) with direct numerical simulations of the basic Eq. (1) (solid line for T and dashed line for M) is also shown. One can see excellent agreement between the simple approach based on solving ODEs and direct numerical simulations. Note that variational method allows also to describe changes of the fast dynamics related to the transformation of the input signal with Gaussian or sech profile to the asymptotic form of the dispersion managed soliton. These changes are adopted by simple recalculations of the parameters C_1 and C_2 through Eqs. (14) and (15).

More generally, we look for the conditions for fixed points by varying the parameters $\langle d\rangle$, K, and C_1. For example, if $\langle d\rangle$ and K are fixed, the coefficient C_2 is determined by the requirement that the solution is periodic (with periodicity length L). Strictly periodic solutions exist only for particular values of C_2 which determine the energy enhancement for a dispersion-managed soliton. Fig. 4 shows how the parameter C_2 (and consequently the energy of an asymptotic pulse) depends on K. Correspondingly, in the insets the variation of C_2 with respect to $\langle d\rangle$ is shown for a fixed value of K for an element of type I. As can be seen from Fig. 4, the energy of the asymptotic pulse (being proportional to C_2) increases with increasing K. This is in accordance with an empirical formula presented in Ref. [19] and our analytical result. An important issue is that the strength of the considered map is bounded from above by some cut-off value K_{cr}. The cut-off parameter K_{cr} decreases with increasing residual dispersion. The occurrence of such a restriction on the strength parameter K means that

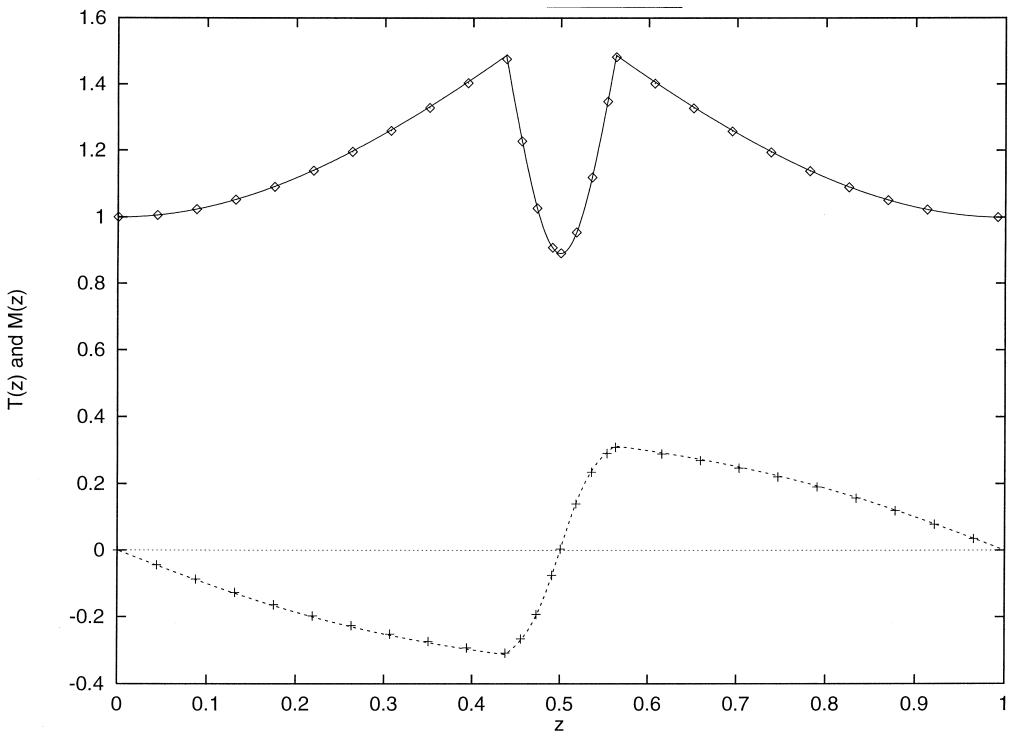

Fig. 3. Variation of the width T and $M = \mu T$, related to the chirp over the (normalized) space coordinate $z = Z/L$ within an element of type I. The parameters $K = 3$, $\langle d \rangle = 0.2$, $C_1 = 0.5$, and $C_2 = 0.2563$ are chosen in such a way that the solution is periodic. It is demonstrated also the comparison of the results obtained by the variational approach (squares for T and crosses for M) with direct numerical simulations of Eq. (1) (solid line for T and dashed line for M).

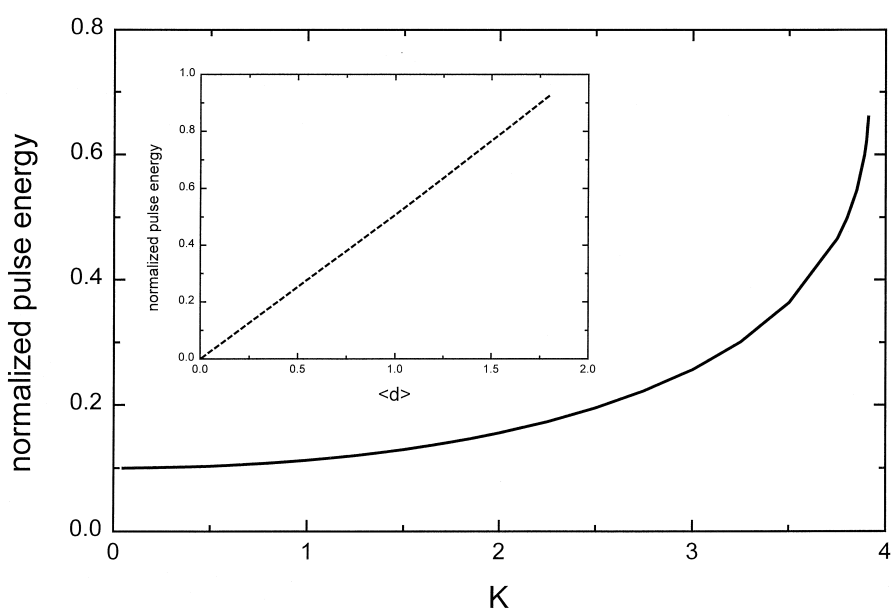

Fig. 4. Condition for a periodic solution in a type I element. Shown is the variation of soliton energy (normalized by $P_0 t_0 2\sqrt{2\pi}$) with: (main picture) the map strength parameter K and (inset) with the residual dispersion $\langle d \rangle$ for the parameters $d_2 = 12$, $C_1 = 0.5$ and $\langle d \rangle = 0.2$ and $K = 0.2$ for the inset.

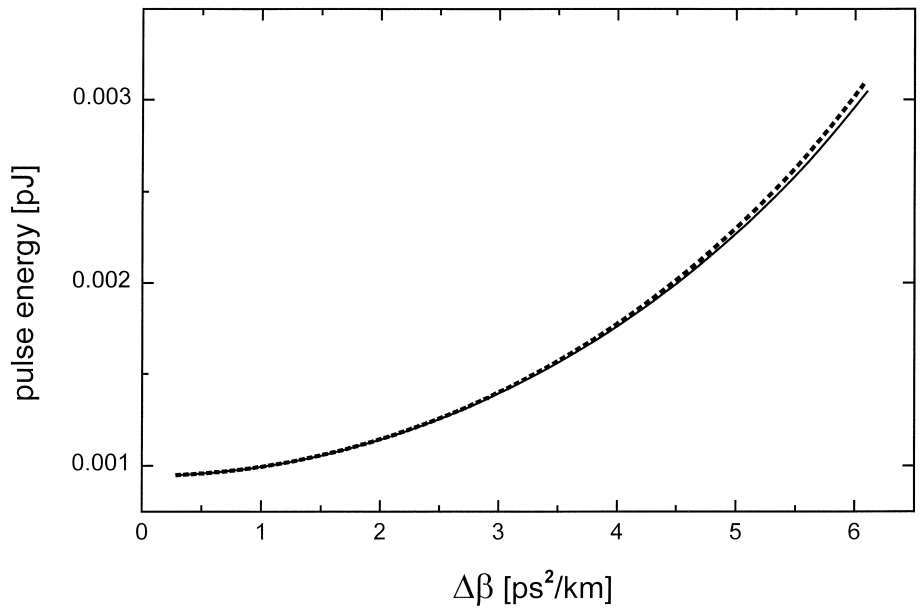

Fig. 5. Comparison between the numerical (solid line) and analytical (dashed line) results for the soliton energy enhancement in a type II element. Shown is the enhancement of the soliton energy with the difference of dispersion of two building fiber pieces $\Delta\beta$ for $\langle\beta\rangle = -0.01$ ps^2/km and $C_1 = 1$.

for a particular system design of type I, with fixed $\tilde{d}_2 > 0$ and $\langle d\rangle = \text{const}$, the group delay parameter for a periodic solution must satisfy the condition

$$\tilde{d}_1 > \frac{-\tilde{d}_2 K_{\text{cr}}}{2\tilde{d}_2 - K_{\text{cr}}}\,. \tag{69}$$

If, however, we keep the relation $\tilde{d}_1 \equiv -\tilde{d}_2$ fixed, no such cut-off occurs. Then the strength parameter K is not bounded from above. In Figs. 5, 6 we compare the results of the numerical solution of Eqs. (12) and (18) and analytical formula (67).

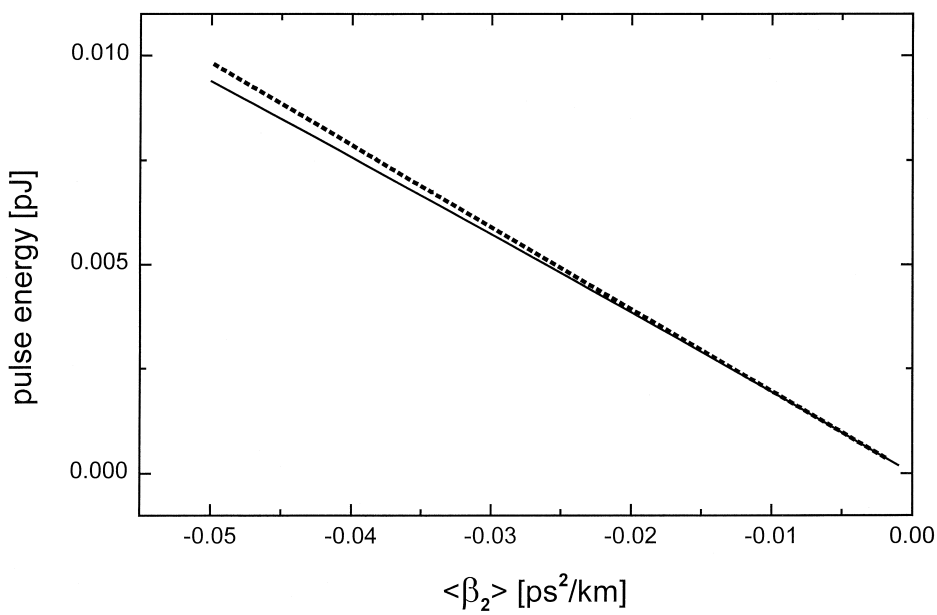

Fig. 6. The same comparison as in Fig. 5, but for the dependence of the soliton energy on the average dispersion $\langle\beta\rangle$ for a fixed $\Delta\beta = 4.4$ ps^2/km.

Solid line is for the numerical solution and dashed line is for the analytical result (67). Fig. 5 shows the dependence of the dispersion-managed soliton energy on the difference between local dispersions of two fibers in the element of type II. In this range of parameters agreement is rather good. Of course, for larger $\Delta\beta$ when the effect of nonlinearity increases (C_2 becomes not small) first order perturbation is not valid and agreement between numerics and Eq. (67) breaks down. In Fig. 6 a similar comparison between numerics and analytical result for the energy dependence on the average dispersion $\langle \beta \rangle$ is shown. We would like to point out that the above analytical description of the energy enhancement is limited by the case of perturbative effects of nonlinearity and residual dispersion (though this limit is rather practical). In summary, we have found a range of system parameters for which the dependence of the power enhancement on map strength and average dispersion can be described analytically.

6. Details of the pulse form

The above description is valid for any localized function f. So far we have characterized f only by two parameters, C_1 and C_2. The form of f has not been specified in more detail, and it seems that this is enough for most practical applications. However, in this section we want to show that the variational method is capable of providing more information on the pulse form. We can use the same variational principle as in Section 3 to analyze the general features of the function f. Let us assume that the asymptotic pulse is an oscillating quasi-soliton, i.e. we suppose that the shape of the pulse is reproduced after one transit through the compensating element. This assumption is justified by several numerical simulations of the time- and space-dependent situation, see, e.g., Refs. [19,28,33]. Let us again start with the ansatz

$$A(z,t) = \frac{1}{\sqrt{T(z)}} f\left[t/T(z)\right] \exp\left(i\lambda z + i\frac{M}{T}t^2\right), \tag{70}$$

where $T(z)$ and $M(z)$ are periodic solutions of Eqs. (12) and (13) with some arbitrary C_1 and C_2. Because any solution of Eq. (1) must realize an extremum of the action S, we can consider now the variational problem $\delta S = 0$ in order to determine the general features of the function f. After averaging the Lagrangian over one period in z, one finds by some simple calculations that the equation for the shape of the asymptotic pulse $f(s)$ is

$$\alpha_1 \frac{\mathrm{d}^2 f}{\mathrm{d}s^2} + \alpha_2 |f|^2 f - kf - hs^2 f = 0, \tag{71}$$

$$h \equiv \alpha_1 C_1 - \alpha_2 C_2, \tag{72}$$

where

$$\alpha_1 = \langle d(z)/T^2 \rangle \tag{73}$$

and

$$\alpha_2 = \langle c(z)/T \rangle; \tag{74}$$

$\langle\ \rangle$ means averaging over one element. Here, k is a parameter (wave number) of the soliton, and α_1, α_2, C_1, and C_2 are constants related to the dispersion map. The procedure to describe the detailed shape of the asymptotic breathing soliton (corresponding to a specific dispersion compensating element) is as follows. First, we find the periodic solutions of Eqs. (12) and (18), i.e. for T and M for arbitrary C_1. Then, the coefficients α_1 and α_2 should be calculated. The next step is to solve Eq. (71) for arbitrary k and C_1. When $\alpha_1 C_1 = \alpha_2 C_2$, the pulse profile is close to that of a fundamental soliton of the cubic nonlinear Schrödinger equation. For the simplest versions of the compensating systems (similar to the studies in Refs. [18,28,19]), our analysis (for different dispersion maps) shows that the parameter h is always negative. In Ref. [38] it has been proved that h is always negative for true periodic solutions of Eqs. (12) and (18). Negative h values correspond to tunneling of the radiation from the central part of the dispersion-managed soliton. The effective potential ($\sim hs^2$ in Eq. (71)) is of nontrapping type in this case. Typical solutions of Eq. (71) show some humps in the tails as can be seen in Fig. 7. The envelope of the oscillatory tails decays very slowly. This steady-state solution can approximate the central part of the asymptotic solution in the nonstationary problem for small h. In this case a slow tunneling of the radiation from the main peak takes place, due to the nontrapping parabolic potential. Numerical simulations show that the tails are not self-similar to the main peak and therefore, the variational approach in the above form is not an optimal way to describe these tails. Note also that the energy of the tails are much smaller than the energy of the main peak for a DM soliton.

The typical three-dimensional plot of the evolution of the dispersion-managed breathing soliton approximated by the self-similar trial function (8) along one section in the type II compensating system is shown in Fig. 8. The pulse broadens in

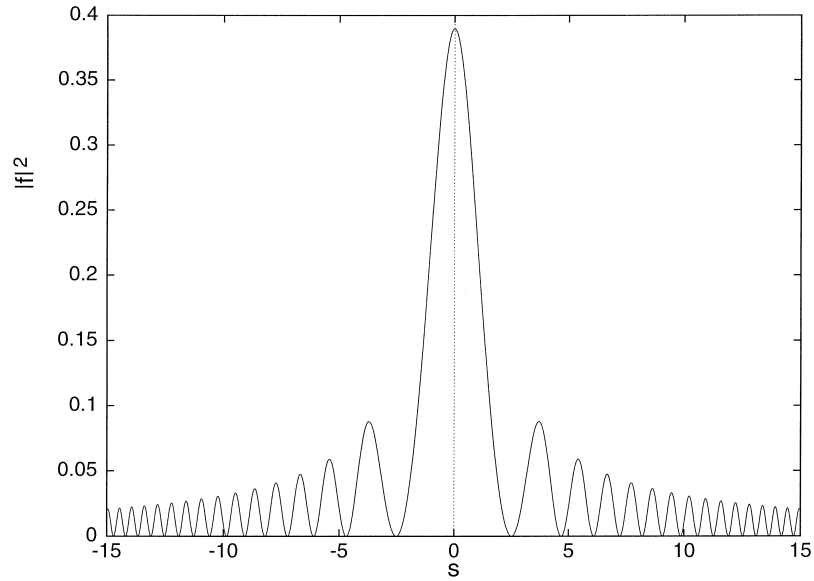

Fig. 7. Typical shape of a solution of Eq. (71).

the first part of the section and acquires chirp; in the middle part (with opposite dispersion) the pulse is compressed and recompressed, in accordance with the evolution of T found from the ODE model; and in the last section the pulse recovers its width and chirp at the end of the cell. The dynamics of the main energy-bearing part of the DM soliton is described with good accuracy by the self-similar structure (8). Far-field tails (that are not seen in Fig. 8) are not self-similar, but their energy is rather small.

An interesting result from the analysis of Eq. (71) is that the mandatory condition of positive (anomalous) average dispersion ($\langle d \rangle > 0$) that provides the existence of the fundamental soliton is changed for a dispersion-managed soliton to the requirement $\alpha_1 > 0$. This means, in particular, that the dispersion-managed soliton can exist even at zero or normal average dispersion. The region where the dispersion-managed soliton can propagate can now be easily found. Including the region where residual dispersion $\langle d \rangle$ is negative (or zero) still allowing soliton propagation. A dispersion-managed soliton can propagate in the region where $\alpha_1 = \langle d/T^2 \rangle > 0$. It should be noted that Eq. (71) has been derived in Ref. [36] by exact averaging of the master Eq. (1). Also this equation describes the shape of the quasi-soliton in a system with programmed chirp and dispersion [37]; and the shape of the soliton propagating in the fiber links with in-line phase filtering as considered in Ref. [39].

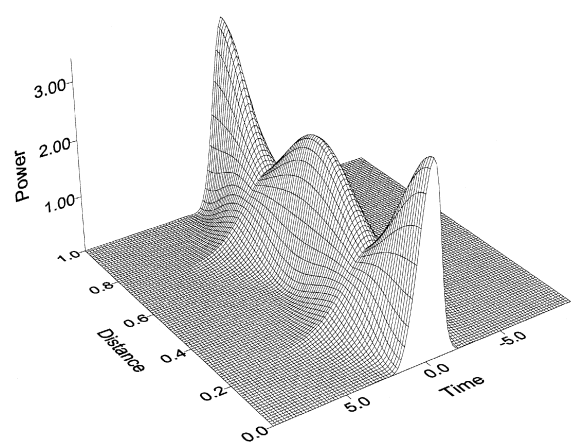

Fig. 8. Self-similar evolution of the dispersion-managed breathing soliton approximated by a trial function (8) along one section in the type II line; $d_1 = -d_2 = d = 5$, $\langle d \rangle = 0.15$.

7. Numerical simulations

In this section we compare results obtained by the variational model given by Eqs. (12) and (18) with pulse dynamics found from direct numerical solution of Eq. (1) for a map of the type II. The compensation scheme is constructed from DSF in the following way: two pieces of DSF with $\beta_2^1 = -2.4$ ps^2/km and the lengths $Z_c = 100$ km each are placed at the beginning and at the end of the element. A piece of DSF with $\beta_2^2 = 2.6$ ps^2/km and the length $L - 2Z_c = 200$ km is placed in the middle. Thus, the total dispersion compensation period is 400 km. Considering an amplification period equal to 40 km (i.e. much smaller than the dispersion compensation period) one can average over the fast oscillations of the power between two consecutive amplifiers. As a result, the inclusion of periodic amplification and dispersion compensation can be handled as separate problems. The parameters used in the calculations are: the nonlinear refractive index $n_2 = 2.6 \times 10^{-20}$ m^2/W, the characteristic time $t_0 = 10$ ps, the operating wavelength $\lambda_0 = 1.55$ μm, the effective fiber area $A_{\text{eff}} = 55$ μm^2. The dimensionless parameters are $\tilde{d}_1 = 5$, $\tilde{d}_2 = -5$ and $\langle d \rangle = 0.2$.

First, we demonstrate that the variational approach gives an excellent approximation of the optical pulse dynamics on one period. Let us define the integral characteristics of the pulse by

$$T_{\text{in}}(z) = \left[\frac{\int t^2 |A|^2 \, \mathrm{d}t}{\int |A|^2 \, \mathrm{d}t} \right]^{1/2}, \quad \frac{M_{\text{in}}(z)}{T_{\text{in}}(z)} = \frac{1}{4} \frac{i \int t (AA_t^* - A^* A_t) \, \mathrm{d}t}{\int t^2 |A|^2 \, \mathrm{d}t}. \tag{75}$$

If an asymptotic pulse is described by Eq. (8) with $T(0) = 1$ then $T_{\text{in}}(z)/T_{\text{in}}(0) = T(z)$ and $M_{\text{in}}(z)/T_{\text{in}}(z) = M(z)/T(z)$. The fast pulse evolution over one element is depicted in Fig. 9. By direct numerical simulations of Eq. (1) we find the values represented by triangles for $T(z)/T(0)$ and by squares for $M(z)$. The corresponding results of the variational approach are shown by solid lines. The agreement is very good. To describe the slow evolution, we consider the stroboscopic dynamics of the pulse peak power and pulse width. In Fig. 10 the long-term (slow) evolution of the pulse characteristics is shown at the ends of the compensation elements (located at $z_k = k; k = 1,2,3,\ldots$ in dimensionless units). The pulse peak powers at the end of sections found by direct simulations of Eq. (1) are represented by squares. The corresponding pulse widths at the end of the elements found from the direct numerical modeling of Eq. (1) are represented by circles. Note that the variational approach predicts straight lines corresponding to the averages. Thus, also the slow dynamics is well represented by the variational prediction.

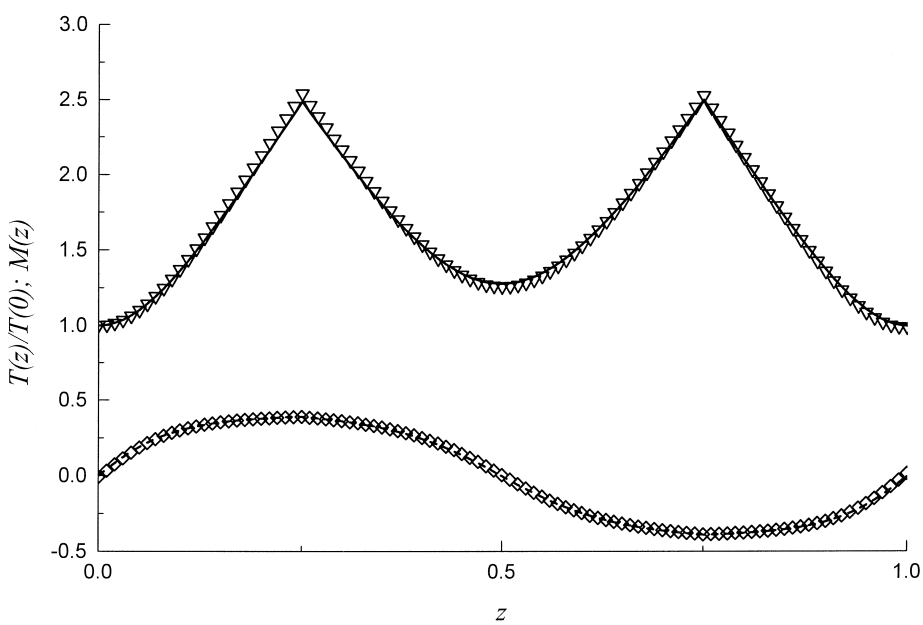

Fig. 9. Comparison of the variational approach with the direct numerical simulation of Eq. (1) in the fast dynamics (over one element). The periodic solution for a type II dispersion map is shown. Triangles for $T(z)/T(0)$ and squares for $M(z)$ correspond to direct numerical simulations of Eq. (1) and the solid lines correspond to the variational approach. Parameters of the map are $d_1 = 5$, $d_2 = -5$, $\langle d \rangle = 0.2$.

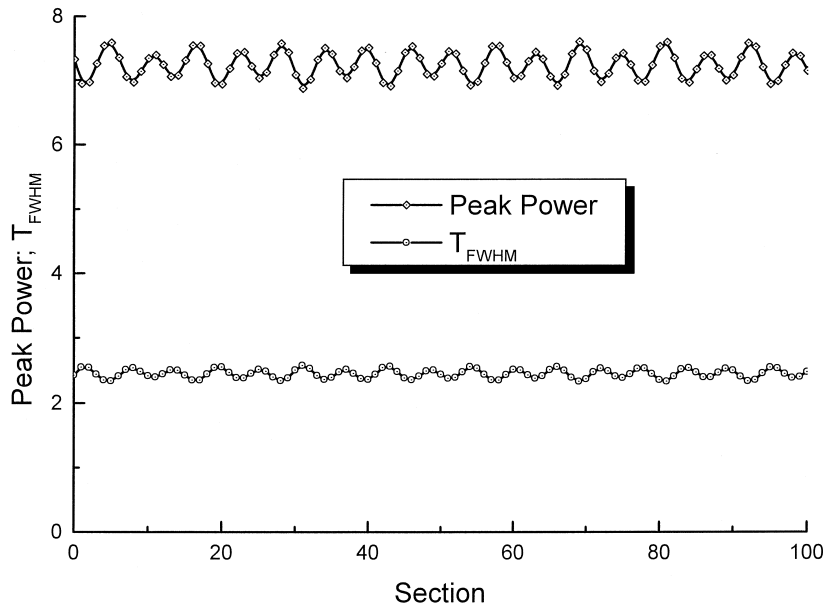

Fig. 10. Comparison of the variational approach with the direct numerical simulation of Eq. (1) in the slow (averaged) dynamics. Direct numerical simulations for the pulse peak power (squares) and the pulse width (circles) at the end of sections are shown. The map parameters are the same as in Fig. 9. Note that the variational approach leads to straight lines.

If the input pulse does not fit the initial conditions for the dispersion-managed soliton as discussed above, then propagating down the fiber it emits radiation that spreads due to dispersion. In many ways the asymptotic pulse dynamics of our model is similar to the asymptotic solutions of the NLS equation studied in Ref. [43]. This dynamics has two basic stages. A ''fast'' separation of the radiative part from the initial pulse and a ''slow'' interaction of the continuous radiation with the main pulse. Further interaction of the continuous radiation with the main pulse results in decreasing oscillations. The corresponding energies of the radiative tail and the main pulse approach constant values [28]. This behavior is in good qualitative agreement with the pulse dynamics in the integrable NLS equation described in Ref. [43].

Continuous radiation leads to a limitation of the bit rate optical links. The source of this limitation is the nonlocal character of the pulse interaction in the bit stream with continuous radiation.

Though variational models are known to be limited (see, e.g. Refs. [42,43]) in the description of some details of nonlinear pulse dynamics, the comparison of the approach developed in this paper with numerical simulations shows that the variational approach is an extremely effective tool for determination of the characteristics of the dispersion-managed soliton. Consequently, the variational method allows to minimize the shedding of the energy into the dispersive part and is an effective way for optimizing the system performance of dispersion-manged optical transmission systems.

8. Summary

In this paper we have analyzed the propagation of an optical pulse in a transmission line with dispersion compensating elements. Characterizing the pulse by a few relevant parameters, we applied a variational principle to determine the variations of the pulse parameters via ordinary differential equations. For piecewise constant dispersion, as it is the case in the dispersion compensating elements, we can solve these differential equations analytically, and thereby the whole problem is reduced to a nonlinear mapping. The fixed points of this mapping determine the operational regime of dispersion compensating elements. The calculations predict the optimal parameters for a long-haul transmission. The procedure is also suitable for analyzing various additional aspects, such as: the basin of attraction of the fixed point in driven dissipative cases, the proper design of the dispersion compensating elements without the restriction of piecewise constant dispersion, the optimized tailoring of the pulse forms, and so on. We have obtained an analytical formula for the soliton power enhancement. This analytical expression is in good agreement with numerical results, in the (practical) limit when residual dispersion and nonlinearity only slightly affect the pulse dynamics over one compensation period. It is verified also that results of the variational approach are in good agreement with results of direct numerical simulations. This proves that the variational method is an effective tool for optimization of dispersion-managed communication lines.

References

[1] L.F. Mollenauer, S.G. Evangelides Jr., H.A. Haus, IEEE J. Lightwave Technol. 9 (1994) 194.
[2] M. Nakazawa, H. Kubota, Electron. Lett. 31 (1995) 216.
[3] L.F. Mollenauer, P.V. Mamyushev, M.J. Neubelt, Optics Lett. 19 (1995) 704.
[4] A. Hasegawa, Y. Kodama, Optics Lett. 15 (1990) 1444; Phys. Rev. Lett. 66 (1991) 161.
[5] K.J. Blow, N.J. Doran, IEEE Photon. Technol. Lett. 3 (1991) 369.
[6] Y.S. Kivshar, K.H. Spatschek, M.L. Quiroga Teixeiro, S.K. Turitsyn, Pure Appl. Optics 4 (1995) 281.
[7] A. Mattheus, S.K. Turitsyn, Pulse interaction in nonlinear communication systems based on standard monomode fibres, in: Proc. ECOC, 1994, vol. 2, p. 37.
[8] F.M. Knox, W. Forysiak, N.J. Doran, IEEE J. Lightwave Technol. 13 (1995) 1955.
[9] R. Kashyap, Photosensitive Optical Fibers: Devices and Applications, Optical Fiber Technology 1 (1994) 17.
[10] D.M. Rothnie, J.E. Midwinter, Electron. Lett. 32 (1996) 1907.
[11] C. Das, U. Gaubatz, E. Gottwald, K. Kotten, F. Küppers, A. Mattheus, C.J. Weiske, Electron. Lett. 31 (1995) 305.
[12] F. Küppers, A. Mattheus, R. Ries, Pure Appl. Optics 4 (1995) 459.
[13] I. Gabitov, S.K. Turitsyn, Optics Lett. 21 (1996) 327; Pisma ZETP 63 (1996) 814.
[14] D. Le Guen, F. Favre, M.L. Moulinard, M. Henry, F. Devaux, T. Georges, 320 Gb/s soliton WDM transmission over 1100 km with 100 km dispersion-compensated spans of standard fibre, in: Proc. ECOC'97, Edinburgh, Postdeadline paper, vol. 5, 1997, p. 25.
[15] M. Nakazawa, K. Suzuki, H. Kubota, E. Yamada, Electron. Lett. 32 (1996) 1686.
[16] M. Suzuki, I. Morita, K. Tanaka, N. Edagawa, S. Yamamoto, S. Akiba, 160 Gb/s (8 x 20 Gb/s) soliton WDM transmission experiments using dispersion flattened fibre and periodic dispersion compensation, in: Proc. ECOC'97, Edinburgh, vol. 3, 1997, p. 99.
[17] M. Suzuki, I. Morita, N. Edagawa, S. Yamamoto, H. Taga, S. Akiba, Electron. Lett. 31 (1995) 2027.
[18] N. Smith, F.M. Knox, N.J. Doran, K.J. Blow, I. Bennion, Electron. Lett. 32 (1995) 55.
[19] N.J. Smith, N.J. Doran, F.M. Knox, W. Forysiak, Optics Lett. 21 (1997) 1981.
[20] J.H.B. Nijhof, N.J. Doran, W. Forysiak, F.M. Knox, Electron. Lett. 33 (1997) 1726.
[21] M. Nakazawa, H. Kubota, K. Sahara, K. Tamura, IEEE Photon. Technol. Lett. 8 (1996) 452.
[22] M. Matsumoto, H.A. Haus, IEEE Photon. Technol. Lett. 9 (1997) 785.
[23] T. Georges, B. Charbonnier, IEEE Photon. Technol. Lett. 9 (1997) 127.
[24] E.A. Golovchenko, A.N. Pilipetskii, C.R. Menyuk, Optics Lett. 22 (1997) 793.
[25] E. Shapiro, S.K. Turitsyn, Phys. Rev. E (Rapid Communications) 56 (1997).
[26] J.N. Kutz, P. Holmes, S.G. Evangelides Jr., J.P. Gordon, J. Opt. Soc. Am. B 22 (1997) 372.
[27] A. Berntson, D. Anderson, M. Lisak, M.L. Quiroga-Teixeiro, M. Karlsson, Optics Comm. 130 (1996) 153.
[28] I. Gabitov, E.G. Shapiro, S.K. Turitsyn, Optics Comm. 134 (1996) 317; Phys. Rev. E 55 (1997) 3624.
[29] G.P. Agrawal, Nonlinear Fiber Optics, Academic, San Diego, 1989.
[30] T.-S. Yang, W.L. Kath, Optics Lett. 22 (1997) 985; T.-S. Yang, W.L. Kath, S.K. Turitsyn, Opt. Lett. 23 (1998) 597.
[31] S. Wabnitz, I. Uzunov, F. Lederer, Photon. Technol. Lett. 8 (1996) 1091.
[32] M. Wald, I. Uzunov, F. Lederer, S. Wabnitz, Phot. Technol. Lett. 9 (1997) 1670.
[33] V.S. Grigoryan, T. Yu, E.A. Golovchenko, C.R. Menyuk, A.N. Pilipetskii, Optics Lett. 22 (1997) 1609.
[34] B.A. Malomed, Optics Comm. 136 (1997) 313.
[35] D. Anderson, Phys. Rev. A 27 (1983) 3135.
[36] S.K. Turitsyn, JETP Lett. 65 (1997) 845.
[37] S. Kumar, A. Hasegawa, Optics Lett. 22 (1997) 372.
[38] A. Hasegawa, Y. Kodama, A. Maruta, Opt. Fiber Technol. 3 (1997) 197.
[39] V.K. Mezentsev, S.K. Turitsyn, Optics Comm. 146 (1998) 225.
[40] E. Shapiro, S.K. Turitsyn, Optics Lett. 22 (1997) 1045; Opt. Fiber Technol. (1998), in press.
[41] E. Shapiro, S.K. Turitsyn, Dispersion-managed soliton in optical amplfier transmission systems with zero average dispersion, to be published in Optics Lett.
[42] D.J. Kaup, T.I. Lakoba, J. Math. Phys 37 (1996) 3442.
[43] E.A. Kuznetsov, A.V. Mikhailov, I.A. Shimokhin, Physica D 87 (1995) 201.